Feedback Control of Biomimetic Exotendon Device for Hand Rehabilitation in Stroke

Dong Hyun Kim, Sang Wook Lee, *Member, IEEE*, Hyung-Soon Park*, *Member, IEEE*

***Abstract*—Many hand exoskeleton devices have recently been developed for hand rehabilitation of stroke survivors, but most hand exoskeletons focused on implementing joint movement driven by individual actuator located at the finger joints rather than considering function of hand muscle-tendons and their coordination. In order to achieve hand rehabilitation targeted on restoration of specific muscle-tendon functions, a biomimetic hand exotendon device (BiomHED) was introduced recently. This paper introduces a ring-type design of exotendon device for easier donning and the design of a feedback control system for controlling posture of the finger. Technical details of the feedback sensor and controller with preliminary experimental results are presented.**

I. Introduction

Stroke often causes serious motor dysfunction which results in long-term disability. While many stroke survivors regain the function of their lower extremities, recovery of the upper limb functionality, especially the function of the distal hand, is slow and limited [1].

In order to help recovering the function of the hand, many rehabilitation devices have been developed. Most of the exoskeleton-type robots, including Rutgers Master II Glove[2], Hand of Hope(Rehab-Robotics Co Ltd. Hong Kong, China) [3], HWARD [4] and others [5, 6], focused on implementing flexion and extension movements of individual finger joints driven by joint actuators rather than functional hand movement driven by muscle-tendon coordination. Recently, a Biomimetic Hand Exotendon Device (BiomHED[7]) was introduced, which is capable of producing functional hand movements by delivering targeted reinforcement of individual hand muscle-tendons. BiomHED used exotendons that replicate the kinetic function of the major muscle-tendons to enable targeted reinforcement of specific muscle-tendon. The initial development of the BiomHED, however, did not include feedback control which requires proper selection of feedback sensor as well as design of MIMO (multiple input multiple output) control system.

Implementation of feedback controller for the BiomHED will allow the device not only to achieve more accurate hand posture but also to identify kinematic deficits resulting from the impairment in the muscle coordination post-stroke. The basic function of feedback control is to achieve targeted hand postures (kinematics) or fingertip force (kinetics) required for conducting various functional hand tasks. In addition, implementation of a feedback controller will allow us to measure additional exotendon force needed to replicate kinematics of the manual task performed by control subjects, which can be used to quantify the degree of impairment of the corresponding muscle-tendon function.

However, implementation of feedback control for the BiomHED presents greater challenges compared to the feedback control for typical exoskeleton-type devices driven by joint actuators. While most exoskeleton devices using electric motors can use decoupled SISO (single-input -single-output) controllers for individual joints, exotendon-type device would require complicated MIMO (multiple-input–multiple-output) controller to account for the coupled behavior between multiple tendons and multiple finger joints. In addition, the actuation in the exotendon device is unidirectional – it only applies force to one direction- while the actuators (i.e., electric motors) of exoskeleton-type device are bidirectional. The unidirectional actuation introduces control challenges especially when there is frequent switching between flexion and extension at a joint.

This paper presents our attempt to improve the BiomHED system by addressing the aforementioned limitations of the system. Specifically, the design of the feedback controller including selection, calibration, and installation of position sensor is presented, as well as the control strategy employed to overcome the control challenges observed in the exotendon-type device. We also improved the design of the exotendon device from the glove-type [7] to the ring-type to improve donning of the device for stroke survivors having severe hand contracture.

II. Device Design

A. Mechanical Re-Design of the BiomHED

To conduct the feedback control and for quick donning, the re-designed BiomHED introduced light weight plastic wire guides which consists of two plastic rings and a custom-designed thimble which guide four exotendons as well as mount the bending sensors which are used to measure the finger joint angle. The exotendons are routed through the plastic wire guide and connected to the servomotors that provide tension.

In order to reduce the complexity of the control without losing the major functions of the finger, BiomHED replicated the kinetic function of four major finger muscle-tendon structures that are identified to be important during finger movements and fingertip force generation in grip tasks. The

This research work is supported by Je Won Research Foundation & National Research Foundation Brain Korea 21 Plus Program.

H. S. Park is with the Department of Mechanical Engineering, Korea Advanced Institute of Science and Technology, Daejeon, Korea(e-mail: hyungspark@kaist.ac.kr).

S. W. Lee is with the Catholic University of America, Washington, DC, USA, and with the National Rehabilitation Hospital, Washington, DC, USA (e-mail: leeb@cua.edu).

D. H. Kim, is with the Department of Mechanical Engineering, Korea Advanced Institute of Science and Technology, Daejeon, Korea(e-mail: bomdon@kaist.ac.kr).

four major finger muscle-tendons include extensor digitorum communis (EDC), flexor digitorum profundus (FDP), and the radial and ulnar interossei (RI and UI).

The kinetic functionality of each muscle-tendon (EDC, FDP, RI, UI) was replicated with four 'exotendons'. The exotendon cable is wrapped around the servomotor axis to exert tension to the cable.

Each exotendon is routed through holes in the ring-shaped guides to resemble the path of the four muscle-tendons (Fig. 1). The first exotendon (FET_1) mimics function of EDC. The second exotendon (FET_2) replicates the function of FDP. The third and fourth exotendon (FET_3, FET_4) replicate the function of RI and UI. FET_3 and FET_4 are merged at the palmar side and connected to a servomotor. Therefore, three motors are used to pull FET_1, FET_2 and $FET_{3,4}$, respectively.

Each guide consists of two plastic pieces that are hinged at a joint for easy and quick donning. All exotendons are fixed at a thimble worn on a fingertip and they are routed through two ring-type guides. The other end of each exotendon has a hook for easier connection to the cables from the remotely located servo motors. Two ring-type guides are open initially with the exotendon cables pre-routed, put on intermediate and proximal phalanges respectively, and closed and locked for being ready for the operation. Inner surface of each ring-shaped guide is covered with sticky cushion to provide comfortable operation and to avoid skin movement.

The custom-designed thimble and ring-type guides also have slits on the dorsal side of the rings for mounting of bending sensors. The slits hold the bending sensors in position while allowing smooth sliding of the thin film-type bending sensors for consistent measurement. The bending sensors would make a wrinkle that distorts angle measurement without the slits that allow sliding of the sensors.

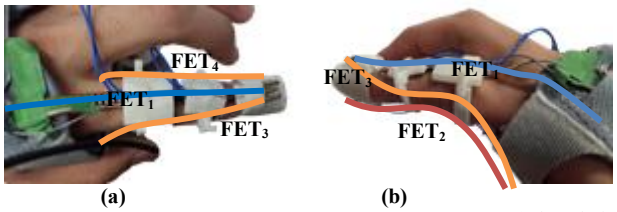

Fig. 1. Light weight finger exotendon device prototype: (a) dorsal view (b) side view

B. Sensor Selection

Among potential candidates for joint sensors including digital encoder, potentiometer, bending sensor, and stretchable PDMS(Polydimethylsiloxane) sensor [8], we excluded the choice of digital encoder and potentiometer since they occupy greater space and their joints need to be aligned with finger joint. We tested durability, consistency and the easiness of installation of the commercial bending sensors and the custom made stretchable PDMS sensor, and the Bend Sensor (one inch long, Flexpoint Inc. Draper, Utah) were selected for measuring distal interphalangeal (DIP) joint and proximal interphalangeal (PIP) joint angles, and the Flex Sensor (four inches long, Spectrasymbol Corp. Salt Lake City, Utah) for the metacarpophalangeal (MCP) joint. The sensors were inserted into slits in the thimble and ring-type guides on the dorsal aspect of the finger (Fig. 2(a)).

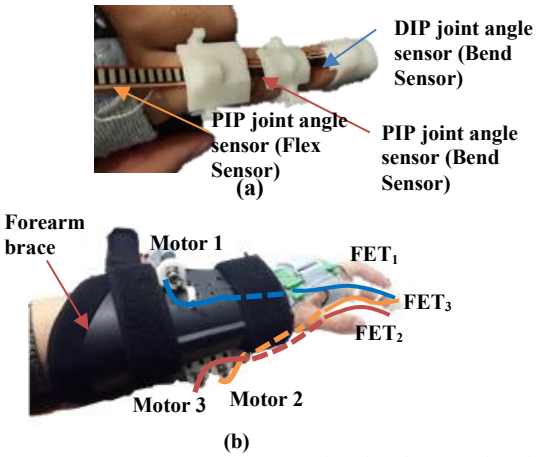

Fig. 2. Sensor and motor location: (a) sensor location (b) motor location

C. Actuator and Actuator mount module

The DC servomotors that pull the exotendons are remotely located on the forearm brace to avoid bulky design at hand and to allow greater room for finger movement (Fig. 2(b)). The exotendon is wrapped around a pulley that is clamped on the motor shaft. As the three brushed DC servomotors (A-max16, Maxon Motor AG, Switzerland) turns, they apply tension to the exotendons (FET_1~FET_4).

The DC motors are operated at current (or torque) control mode by using commercial motor drivers (ESCON 36/2, Maxon Motor AG, Switzerland) to directly apply desired tension force to the exotendons. The motor driver controls for desired torque which is proportional to the voltage command input to the motor driver. By controlling the torque of the motor we can apply desired tension at each exotendon.

Motor drivers and DC servomotors with the cables and hooks were mounted on a commercial forearm brace (DR-W012, Dr. Med Co. South Korea). During experiments, subjects first put on the forearm brace, then the fingertip thimbles and ring-type guides with the pre-routed exotendons. Finally, the exotendons and the cables from motors are connected for operation.

III. Control

A. Sensor Calibration

Calibration of the bending sensors was performed to transform the voltage signal from the sensor to the joint angles of the finger. After placing the sensors on the finger joints, we measured the sensor outputs when each individual joint angle was increased with a small increment (5 to 10 degrees). The equation fitting the curve between the joint angle and voltage signal (Fig 3.) was obtained by using Matlab polyfit function. Eventually, the equation derived from the calibration process was used to transform the voltage signal to each joint angle of the finger.

Although DIP and PIP joints used identical sensors, different equations are obtained because of the different geometry of sensor installation at each joint. As shown in Fig. 3 (a) and (b), the voltage outputs from the one inch long Bend Sensor (Flexpoint Inc. Draper, Utah) saturated at 60 degrees of flexion due to the inherent relation between deflection and voltage output of the sensor. The other four inch long Flex sensor (Spectrasymbol Corp. Salt Lake City, Utah) had linear equation between the voltage output and the joint angle

within the joint range of motion (Fig. 3(c)). The equations derived from this test will be different across subjects, because the sensor signal will change by different finger size and moment arm.

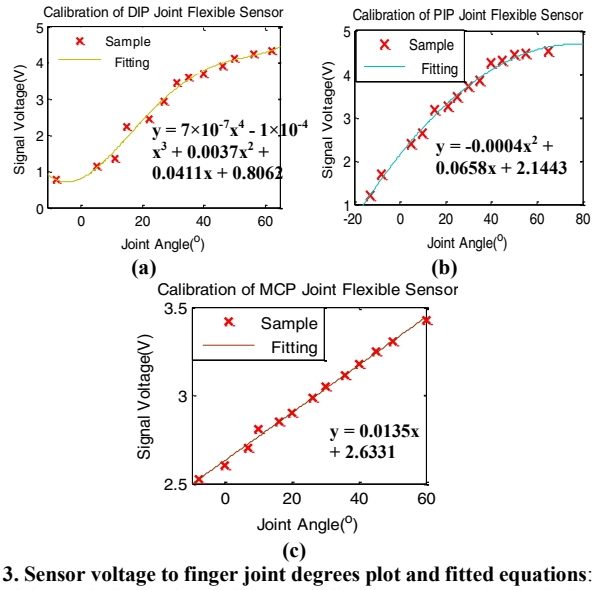

Fig 3. Sensor voltage to finger joint degrees plot and fitted equations: (a) DIP joint angle fitting (b) PIP joint angle fitting (c) MCP joint angle fitting

B. Control Design

1) Transformation Matrix between Exotendon Tension and Angular Displacement

The transformation of the exotendon force to the angular displacement of the joint was experimentally identified from the measured joint angular displacements under individual exotendon loading conditions. [7]

The neutral finger posture (a finger posture that could be maintained without activating the muscle) for each test was measured and set as a reference finger configuration (FET_1 test: DIP joint angle 25°, PIP joint angle 45°, MCP joint angle 45°, FET_2 and $FET_{3,4}$ test : DIP joint angle 5°, PIP joint angle 30°, MCP joint angle 15°). At a reference finger configuration constant control input voltage is applied to a DC servomotor to apply constant tension force to an exotendon of interest while the other DC servomotors are turned off. The changes in joint angles caused by the constant tension force are obtained at every 0.3 volt which corresponds to 0.1953N for FET_1 and every 0.1 volt which corresponds to 0.0651N for FET_2, and $FET_{3,4}$.

The identical test procedure was applied for each exotendon while the other exotendons were disconnected from the motor. From the data collected, we obtained the approximated linear slope between the joint angles and control input voltages (or exotendon forces). The following relation holds because we forced only one exotendon for each tests.

$$\theta_i = \frac{\Delta\theta_i}{\Delta V_j} V_j + V_{joffset}\,, \quad V_j = \frac{\Delta V_j}{\Delta\theta_i}\theta_i - \frac{\Delta V_j}{\Delta\theta_i} V_{joffset}, \quad (1)$$

Where, θ_i*: ith joint angle,* $(i = 1:DIP, 2:PIP, 3:MCP)$

V_j*: jth exotendon control input voltage*

$(j = 1:FET_1, 2:FET_2, 3:FET_{3,4})$

$V_{joffset}$ *: jth exotendon control input voltage offset*

The 3x3 matrix consisting of the linear slopes $(\Delta V_j/\Delta\theta_i)$ are summarized in TABLE I

TABLE I.

LINEAR COEFFICIENTS OBTAINED FROM THE LINEAR FITTING OF THE CONTROL INPUT VOLTAGE TO RESULTANT FINGER JOINT ANGLE DATA(V/°)

Exotendon (Voltage)	**Joint (degree)**		
	DIP	***PIP***	***MCP***
FET_1	-0.0451	-0.125	-0.0452
FET_2	0.0119	0.0288	0.0143
$FET_{3,4}$	-0.107	0.0782	0.0497

From the data in Table I, the following equation is obtained.

$$\begin{bmatrix}\Delta V_1\\ \Delta V_2\\ \Delta V_3\end{bmatrix} = \frac{1}{3}\mathbf{T}\begin{bmatrix}\Delta\theta_1\\ \Delta\theta_2\\ \Delta\theta_3\end{bmatrix}, \quad \textbf{(2)}$$

$$\textbf{where, } \mathbf{T} = \begin{bmatrix}-0.0451 & -0.125 & -0.0452\\ 0.0119 & 0.0288 & 0.0143\\ -0.107 & 0.0782 & 0.0497\end{bmatrix}$$

and $\Delta\theta_1$, $\Delta\theta_2$, and $\Delta\theta_3$ denote for changes in DIP, PIP, and MCP joint angles whereas ΔV_1, ΔV_2, and ΔV_3 stand for the changes in voltage input of FET_1, FET_2, and $FET_{3,4}$. 1/3 in front of **T** from Eq. (2) is multiplied to take average of the control voltage input change respect to each joint angle changes, because the joint angle changes are actually coupled to the control input voltage.

Eq. (2) can also relate the exotendon force and the joint torques assuming that the angular perturbation is proportional to the joint torque.

2) Control Algorithm

A basic MIMO (multi-input multi-output) proportional control algorithm is constructed by using Eq. (2). The angular perturbation vector $\Delta\boldsymbol{\theta} = [\Delta\theta_1, \Delta\theta_2, \Delta\theta_3]$ is replaced with the position error vector, $\mathbf{E} = [e_1, e_2, e_3]$, where e_1, e_2, and e_3 denote the position error at DIP, PIP, and MCP joints respectively. The control input vector, $\mathbf{V} = [V_1, V_2, V_3]$ is obtained as the following proportional control based MIMO controller with K_P as a constant proportional control gain.

$$\mathbf{V} = K_p\mathbf{T}\cdot\mathbf{E} \;\; (V_1, V_2, V_3 > 0) \;\; \textbf{(3)}$$

Since the actuators cannot apply compressive force input, Eq. (3) holds for the positive control input values which corresponds to tensional forces. When Eq. (3) returns negative control inputs for a certain set of position errors, the negative control input is considered as loosening of the corresponding exotendon not to resist against tensions at the other exotendons. This was implemented by setting a small negative voltage threshold that is barely enough to remove residual tension at the exotendon but is not enough to continuously rotate the servomotor to negative direction. Additionally to prevent excessive control input voltage from the feedback control for safety maximum positive limit (or maximum tension) was set. The A/D and D/A conversion and the control logic was implemented using PCI-6229 (National Instruments Co., Austin, TX) and a custom Labview Program (National Instruments Co., Austin, TX) which runs at 1kHz.

IV. PERFORMANCE EVALUATION

A. Experimental Procedure

The performance of the controller was tested for the following three finger target configurations: 1) full extension (DIP joint angle : 0°, PIP joint angle : 0°, MCP joint angle : 0°), 2) full flexion (DIP joint angle : 45°, PIP joint angle : 50°,

MCP joint angle : 50°) and 3) flexion of MCP joint and PIP joint, and slight extension of the DIP joint(DIP joint angle : 0°, PIP joint angle : 50°, MCP joint angle : 50°).

The ring-type exotendon device was put on a healthy subject (25 years old, Male) who was informed and consented. The subject was asked to relax his hand throughout the experiment. The desired joint angles were set on the Labview program and the control was triggered by a start button on the program. Each set of the three target finger configurations was tested and the joint angle data were collected at 1kHz.

B. Results

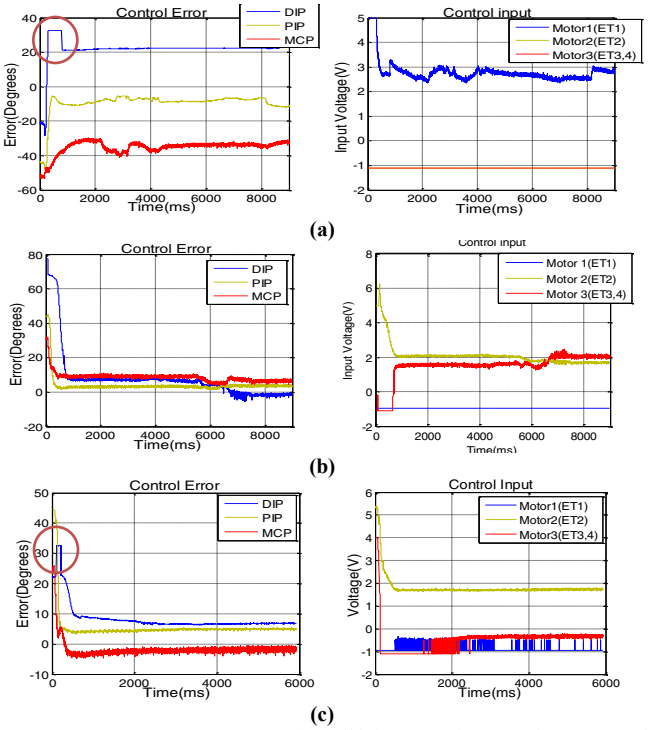

Fig.4. Joint control error graph: (a) Full joint extension experiment control error & control input, (b) Full joint flexion experiment control error & control input, (c) PIP, MCP flexion and DIP extension experiment control error & control input. The step-like response in the DIP joint (circled in Fig (a) and (c)) was cause by sensor error at the small joint angle range (below -5°).

Fig. 4 shows the errors in DIP, PIP, MCP joint angle for the three sets of finger posture.

1) *Full joint Extension*

The errors in joint angles decreased; however, the steady-state error was significant (average 20°).

2) *Full joint Flexion*

The errors decreased with the average steady-state error of 7°.

3) *Flexion of MCP and PIP, and Extension of DIP*

The errors decreased and the average error was 5°.

The amount of steady-state error was considerable for the configuration 1) whereas the joint flexion involved smaller steady state errors.

V. Discussion & Conclusion

The purpose of the study was to improve the design of exotendon device for easier donning and, more importantly, to implement position sensors that allow precise position control of the device.

By employing ring-type guides, we could achieve easier and quicker donning of the device. We expect that the use of ring-type guide would greatly facilitate the donning process of the device for patients, as the device can be worn without fully extending fingers of patients, which is often extremely difficult and very time-consuming.

Some limitations of the device were observed. Although a simple proportional MIMO feedback controller designed based on the identified force-joint angle transformation algorithm was able to change the finger posture close to the aimed posture, significant steady state errors were observed for some target postures (i.e., full finger extension). It is not surprising to have steady state errors with the proportional feedback only, but the steady state errors were particularly large for the fully extended posture. This might be due to the increased stiffness of the finger joints when they are fully extended. Therefore, we plan to implement PI (proportional and integral) controller to reduce steady-state errors, with the identification of the system and the pre-study of the stability when PI control is implied.

The controller was only tested while the user was relaxed; in the future, for the realistic rehabilitation tasks we plan to implement interactive feedback controller that assists the user as needed when users actively moves toward target posture, by continuously monitoring the amount of assistance needed (i.e., current measurement).

While testing the device, hyperextension of the DIP joint occurred at relatively small tension force. This is due to the thimble design causing large moment arm of the FET_1 and $FET_{3,4}$. Improvement in mechanical design needs to be made to better mimic the human hand muscle-tendon structure. For practical use in a clinical setup, a systematic procedure for calibration of the bending sensors and transformation matrix estimation will need to be developed. While it is challenging to implement feedback control in the exotendon-type device, it has a potential to enhance the effectiveness of hand rehabilitation. By using the feedback control it is possible to identify which exotendon requires greater assistance to attain an aimed posture so that we can target on a specific muscle-tendon during the rehabilitation. It will also allow us to design muscle-tendon coordination pattern during specific tasks.

VI. Reference

[1] Twitchell, T.E., *The restoration of motor function following hemiplegia in man.* Brain, 1951. **74**(4): p. 443-80.

[2] Bouzit, M., et al., *The Rutgers Master II - New design force-feedback glove.* IEEE-ASME Trans Mechatronics, 2002. **7**(2): p. 256-263.

[3] Ho, N.S., et al., *An EMG-driven exoskeleton hand robotic training device on chronic stroke subjects: task training system for stroke rehabilitation.* IEEE Int Conf Rehabil Robot, 2011. **2011**: p. 5975340.

[4] Takahashi, C.D., et al., *Robot-based hand motor therapy after stroke.* Brain, 2008. **131**(Pt 2): p. 425-37.

[5] Cempini, M., et al., *Kinematics and design of a portable and wearable exoskeleton for hand rehabilitation.* IEEE Int Conf Rehabil Robot, 2013. **2013**: p. 6650414.

[6] Jones, C.L., et al., *Design and Development of the Cable Actuated Finger Exoskeleton for Hand Rehabilitation Following Stroke.* IEEE-ASME Trans Mechatronics, 2014. **19**(1): p. 131-140.

[7] Lee, S., K. Landers, and H. Park, *Development of a Biomimetic Hand Exotendon Device (BiomHED) for Restoration of Functional Hand Movement Post-Stroke.* IEEE Trans Neural Syst Rehabil Eng, 2014. **PP**(99): p. 1-1.

[8] Jeong, G.S., et al., *Solderable and electroplatable flexible electronic circuit on a porous stretchable elastomer.* Nat Commun, 2012. **3**: p. 977.